Chromosomal instability and phenotypic plasticity during the squamous-spindle carcinoma transition. Association of a specific t(14;15) with malignant progression

Mar Pons,[1] Juan C. Cigudosa,[2] Sandra Rodríguez-Perales,[2] José L. Bella,[3] Cristina González,[1] Carlos Gamallo,[1,4] and Miguel Quintanilla[*,1]

[1]*Instituto de Investigaciones Biomédicas Alberto Sols, Consejo Superior de Investigaciones Científicas (CSIC)-Universidad Autónoma de Madrid (UAM), Arturo Duperier 4, 28029-Madrid, Spain;* [2]*Cytogenetics Unit, Centro Nacional de Investigaciones Ocológicas (CNIO), Madrid, Spain;* [3]*Department of Biology, Facultad de Ciencias, UAM, Madrid, Spain; and* [4]*Department of Pathology, Hospital Universitario de la Princesa, Facultad de Medicina, UAM, Madrid, Spain.*

[*] Correspondence: Dr. Miguel Quintanilla
E-mail: mquintanilla@iib.uam.es
Telephone: 34-91-5854412
Fax: 34-91-5854401

Running title: t(14;15) and mouse skin tumor progression

Key words: malignant progression, H-Ras, INK4a, chromosomal instability, T(14;15)

Abstract

In mouse epidermal carcinogenesis, the latest stage of malignant progression involves the transition from squamous cell carcinoma to a highly aggressive type of tumor with spindle morphology. In this work, we have isolated a minor epithelial cell subpopulation (CarC-R) contained in the highly malignant spindle carcinoma cell line CarC. CarC-R exhibited a drastic reduction in tumorigenicity when compared with CarC, but CarC-R-induced tumors were mainly sarcomatoid, although they subsequently reverted to the epithelial phenotype when tumor explants were recultured *in vitro*. Several single cell clones with either stable epithelial or fibroblastic phenotypes were isolated from an explanted CarC-R tumor (CarC-RT). All these cell lines contained the same specific point mutation in *H-Ras* codon 61, but while CarC spindle cells had lost the normal *H-Ras* allele it was retained in CarC-R and CarC-RT-derived cell lines. Furthermore, CarC cells have inactivated *p16INK4a* and *p19INK4a/ARF* transcription, while CarC-R and CarC-RT clones expressed *p19* mRNA and protein but not *p16*. Altogether, these results suggest that CarC-R represents a precursor stage to CarC in malignant progression. Spectral karyotyping analysis revealed that CarC-R was highly aneuploid and contained many chromosomal abnormalities. In contrast, CarC had a diploid or tetraploid modal chromosome number and contained a specific T(14;15) translocation in all of the analyzed metaphases. The T(14;15) translocation was present in only a minority (1.9%) of CarC-R cells, but it was widely spread in CarC-RT and its derived cell clones, regardless of their epithelial or fibroblastic phenotype, indicating that T(14;15) segregates with malignancy.

Words: 246

Introduction

It is believed that cancer arises from the stepwise accumulation of protooncogene and tumor suppressor gene mutations, and the progressive alteration of gene expression. One of the best characterized model systems with respect to genetic changes that contribute to tumor initiation, tumor outgrowth and malignant progression is the mouse skin model of chemical carcinogenesis (Yuspa *et al*., 1994, Frame *et al*., 1998). Numerous benign papillomas develop on the dorsal skin of mice initiated by 7, 12-dimethylbenz(*a*)anthracene (DMBA) and promoted by 12-*O*-tetradecanoylphorbol-13-acetate (TPA). A small number of papillomas progress to form squamous cell carcinomas (SCCs), and spindle cell carcinomas (SpCCs) evolve late in carcinogenesis (Klein-Szanto *et al*., 1989), associated with down-regulation of epithelial differentiation markers, such as E-cadherin and keratins, and the induction of mesenchymal components, such as vimentin (Navarro *et al*., 1991; Ruggeri *et al*., 1992; Diaz-Guerra *et al*. 1992, Stoler *et al*., 1993). This phenomenon, referred to as epithelial-mesenchymal transformation (EMT), is considered a crucial event in late stage tumorigenesis leading to a highly aggressive and metastatic type of tumor, and has also been observed in human cancer (Akhurst and Balmain, 1999; Thiery, 2002; Gotzmann *et al*., 2004).

In the mouse skin carcinogenesis model, a specific activating A-T mutation at codon 61 of the *H-Ras* gene is involved in initiation of carcinogenesis (Quintanilla *et al*., 1986), and amplification/overexpression of the mutant *H-Ras* gene or loss of the remaining wild-type *H-Ras* allele is associated with malignant progression (Quintanilla *et al*., 1986; Bremner and Balmain, 1990; Bianchi *et al*., 1990; Rodriguez-Puebla *et al*., 1999). Specifically, in cases where both squamous and spindle cell components could be identified within the same tumor, both components had the same DMBA-specific *H-*

Ras gene mutation, but the spindle cell component showed a higher mutant to normal gene ratio (Buchmann *et al*., 1991). This, together with the demonstration that both epithelial and spindle cell types share the same point mutations in both alleles of *p53*, a gene whose inactivation occur in about 40% of SCCs, but not in premalignant papillomas (Burns *et al*., 1991), provided a conclusive proof that SpCCs derive from pre-existing SCCs. In addition, it was found that loss or missregulation of the *INK4* locus encoding the cell cycle regulators p15INK4B, p16INK4A and p19INK4A/ARF correlated with the SCC-SpCC transition (Linardopoulos *et al*., 1995). These genetic alterations might drive the spindle transformation in cooperation with other epigenetic events, such as those triggered by transforming growth factor-β (TGF-β) signalling pathways (Akhurst and Balmain, 1999).

Aneuploidy –that is, an imbalance in the normal diploid complement of chromosomes- and chromosomal aberrations are hallmarks of experimental and human cancer. They occur early in tumor formation and increase with tumor progression, suggesting they can play a role in both tumor development and malignancy (Pihan and Doxsey, 1999; Rajagopalan *et al*., 2003; Grady, 2004). In mouse skin carcinogenesis, aneuploidy and chromosomal abnormalities segregate with progressive dysplasia during malignant conversion from papillomas to SCCs (Conti *et al*., 1986; Aldaz *et al*., 1987), and trisomies of chromosome 7 (where the H-Ras gene locus is located) and chromosome 6 have been found in aneuploid papillomas (Aldaz *et al*., 1989).

In this article, we have identified a precursor cell subpopulation (CarC-R) within a highly aggressive spindle carcinoma cell line (CarC). CarC-R cells are epithelial in culture and weakly tumorigenic in nude mice, but produce highly undifferentiated carcinomas *in vivo*. CarC-R cells are aneuploid and exhibit a high degree of chromosomal instability. In contrast, CarC cells have a diploid or tetraploid modal

number of chromosomes and are genetically more stable than CarC-R. A specific reciprocal chromosomal translocation T(14;15), which is associated with malignant progression, was characterized in CarC-R and CarC cells by spectral karyotyping analysis (SKY) and fluorescence *in situ* hybridization (FISH).

Results

The spindle carcinoma cell line CarC contains epithelial cells that exhibit phenotypic plasticity *in vivo*

The CarC cell line was developed from a poorly differentiated mouse skin carcinoma induced by initiation with DMBA and promotion with TPA (Bremner and Balmain, 1990). CarC cells are spindle-shaped in culture, and produce highly anaplastic spindle carcinomas upon injection in nude mice (Diaz-Guerra *et al*., 1992, Buchmann *et al*., 1991). Although CarC cell cultures have maintained a fibroblast-like appearance for more than 10 years (Figure 1), occasionally we observed the presence of isolated cells with an epithelial morphology in routine experiments in which CarC cells were passed at a high dilution. Thus, we isolated an epithelial cell subpopulation (CarC-R) from a late passage (p. > 50) CarC cell culture seeded at low density (Figure 1). CarC-R cells were grown, frozen, and studied as a separate cell line. Characterization of protein differentiation markers revealed that CarC-R cells synthesize E-cadherin and keratins, while the expression of these epithelial protein markers was not detected in CarC cell lysates (*Supplementary Figure 1*). Furthermore, E-cadherin in CarC-R cells was correctly located at cell-cell junctions, suggesting that it is actively mediating cell-cell interactions. CarC-R cells have been found to maintain a stable epithelial phenotype for at least 40 passages.

The tumorigenic properties of CarC and CarC-R cells were compared after transplantation in nude mice. CarC cells gave rise to highly aggressive spindle tumors (Figure 2a, c) at all injection sites (6 out of 6) with short latencies (8-14 days). In contrast, CarC-R cells produced tumors in only 33% of injection sites (2 out of 6) after long latency periods (35-56 days). Histological examination of CarC-R tumors revealed that they were highly undifferentiated, with large areas exhibiting an apparent spindle morphology and small regions (< 5%) containing epithelial cells with no squamous component (Figure 2b, d). The fact that CarC-R cells switched from an epithelial phenotype *in vitro* to a mesenchymal phenotype when placed into a subcutaneous environment *in vivo* suggested that they were phenotipically plastic, able to undergo a reversible EMT *in vitro* and *in vivo* (Portella *et al*., 1998). Indeed, when a cell line (CarC-RT) was derived from an explanted CarC-R tumor, it exhibited a mixed morphology containing cells of both epithelial and fibroblastic appearances, that tended to present a predominant epithelial morphology when the culture was propagated. As expected, CarC-RT cells exhibited higher tumorigenic properties than CarC-R, inducing tumors at all injection sites (4 out of 4) with latency periods close to that of CarC (16-29 days). Nevertheless, tumors induced by CarC-RT cells were not completely spindle, but presented similar phenotypes as those of CarC-R (data not shown). Several single-cell clones that exhibited stable (at least for 20 passages) epithelial (E1, E4, E2) and fibroblastic (F2, F3, F4, F5) phenotypes were isolated from an early-passage CarC-RT cell culture (Figure 1, see also *Supplementary Figure 1*).

Characterization of *H-Ras, p53 and INK4a* genetic alterations

The CarC cell line was reported to contain a characteristic DMBA-associated A-T mutation in the codon 61 of the *H-Ras* gene and to have lost the normal *H-Ras* allele

(Bremner and Balmain, 1990; Buchmann *et al*., 1991). The *H-Ras* codon 61 mutation gives rise to a restriction site for *XbaI* enabling an easy verification of the mutation by the presence of two novel restriction fragments after digestion of the DNA with the enzyme (Quintanilla *et al*., 1986). We analyzed the status of *H-Ras* in CarC and the other cell lines by RT-PCR, using primers that amplify a 400-bp sequence containing the codon 61. The amplified cDNA fragments were fractionated in a gel before and after digestion with *XbaI*. The PDV squamous carcinoma cell line containing an identical codon 61 mutation at *H-Ras* as CarC, but retaining the normal *H-Ras* allele (Quintanilla *et al*., 1991), was used as a control. All of the cell lines exhibited the same *XbaI* polymorphism, but CarC-R and CarC-RT-derived cell clones expressed increased normal to mutant ratios of *H-Ras* when compared with CarC (Figure 3a). In this latter cell line, although most of the amplified cDNA was digested by the enzyme, a faint band migrating to the normal position was observed after a careful inspection of the gel. This DNA was amplified by PCR and identified as normal *H-Ras* by sequencing (data not shown). These results suggest that CarC-R represents a small subpopulation of CarC cells that retain the normal *H-Ras* allele. All of the CarC-RT-derived clones expressed normal and mutated *H-Ras* transcripts irrespective of their phenotype, although the ratio of normal to mutated expression tended to be lower in the fibroblastic clones, particularly in the clone F2.

CarC cells have also been reported to have deleted the genes encoding the cyclin-dependent kinase inhibitors p15INK4b and p16INK4a, an event associated with the late spindle stage of tumor progression in skin carcinogenesis (Linardopoulos *et al*., 1995). The locus *INK4a* is also transcribed into a second alternate mRNA, which originates from an independent first exon, encoding p19ARF (Quelle *et al*., 1995). To analyze the status of the *INK4a* locus in the cell lines, we studied the expression of *p16*

and *p19* by RT-PCR and Western blotting. None of the cell lines expressed *p16* mRNA (Figure 3b) or protein (Figure 3c). However, while no expression of *p19* could be detected in CarC, significant levels of *p19* transcripts and protein were found in CarC-R and CarC-RT-derived cell lines (Figure 3b, c). These results suggest that spindle CarC cells have inactivated the entire *INK4a* locus while CarC-R and its derived cell lines might contain *INK4a* alterations that inactivate *p16*, but not *p19* gene expression. Since silencing of the *p16 INK4a* promoter by methylation has been found in a significant fraction of human tumors (Ruas and Peters, 1998; Serrano, 2000), we tested the effect of the methyltransferase inhibitor 5-aza-2'-deoxycytidine (5-aza-dC) on *p16* expression. Western blot analysis showed that p16 protein was markedly up-regulated in CarC-R, but not in CarC cells, after a 48 h treatment with the drug (Figure 3d), indicating that inactivation of *p16* gene transcription in CarC-R cells occurs by aberrant methylation of the promoter.

We also studied the status of the *p53* gene in the cell lines. To this aim, exons 3-9 of the *p53* sequence were amplified by RT-PCR and the resulting fragments purified and directly sequenced. This region contains the highly conserved DNA-binding core, where almost all mutations found in tumors occur (Vousden and Lu, 2002). No change could be detected in CarC, CarC-R and CarC-RT-derived cell clones respect to the normal sequence (Table 1), while an ATG to GTG point mutation at codon 234 was found in PDV carcinoma cells, as previously described (Burns et al., 1991).

Finally, in order to rule out the possibility that CarC-R represented some contaminating cells in the CarC cell line, we performed a microsatellite marker polymorphism analysis. Three chromosome 1 (D1Mit294, D1Mit383, D1Mit15) and two chromosome 12 (D12Mit199 and D12Mit180) microsatellite markers were

amplified by PCR using specific markers. As shown in *Supplementary Figure 2*, all CarC, CarC-R, F2 and E2 cell lines showed the same pattern of allelic bands.

Characterization of chromosomal abnormalities by spectral karyotyping

Karyotypic analysis of the cell lines revealed that CarC had a diploid or tetraploid modal chromosome number (Figure 4) and most of the aneuploid cells with non-modal chromosome numbers were near-diploid (40-50), near-tetraploid (71-90) or near-octaploid (close to 160). In contrast, CarC-R and CarC-RT-derived cell clones were highly aneuploid. CarC-R, with a mode of 66 chromosomes, was highly homogeneous with regard to the karyotype of individual cells, since about 72% of the cells had 61-70 chromosomes (Figure 4). Clones derived from CarC-RT were more heterogeneous than CarC-R and had modal chromosome numbers ranging from 84 to 102 (data not shown).

In order to study whether specific chromosomal aberrations correlated with the phenotype or tumorigenic characteristics of the cell lines, we carried out a SKY analysis in CarC, CarC-R and two clones of each phenotype, either epithelial or fibroblastic (Table 2). All metaphases analyzed in CarC showed the same T(14;15) reciprocal translocation (Figure 5a, b), and about 25% of the cells had in addition a T(11;19) translocation. The T(14;15) translocation was found to segregate with tumors induced by CarC in nude mice (data not shown). While these were the only significant chromosomal aberrations found in CarC cells, CarC-R and CarC-RT-derived clones exhibited a wide variety of chromosomal abnormalities with the presence of Robertsonian translocations, deletions, insertions, amplifications, and gains and losses of chromosomes (Table 2 and Figure 5c). No specific alteration associated with either the epithelial or the fibroblastic phenotype was observed in the cell clones.

Interestingly, we were unable to detect the T(14;15) translocation in CarC-R cells with this method, even though we increased the number of analyzed metaphases up to 63. However, T(14;15) was recurrent in all of the studied CarC-RT-derived cell clones (Table 2). Since CarC-RT cells come from a tumor produced by CarC-R in a nude mouse after a long latency period, these results suggested that T(14;15) should be present in a small subpopulation of CarC-R cells that was selected *in vivo* during tumor formation.

t(14;15) segregates with tumorigenicity

To confirm the above hypothesis, we carried out a FISH approach to analyze specifically the T(14;15) translocation in a higher number of CarC-R metaphases. Dual color FISH combining bacterial artificial chromosome (BAC) probes mapping at regions C, D1, D3 and E3 of chromosome 15 (Figure 6a) was then performed in CarC-R, CarC-RT and CarC cells. As expected, most of CarC-RT and CarC metaphases contained a translocated chromosome 15 (Table 3), while it was present in only a small proportion of CarC-R cells (Table 3 and Figure. 6b). In all cases, the breakpoint in chromosome 15 was between regions D1 and D3, again indicating a common origin for all of these cell lines. To confirm that a portion of chromosome 15 was swapped with chromosome 14, we chose a BAC probe mapping at region A3 close to the chromosome 14 centromere, together with BACs C and E3 of chromosome 15 (Figure 6c). The A3 probe gave a diffuse spot (green) after hybridization, enabling distinction between this region in chromosome 14 and region C from chromosome 15. The finding of a translocated product containing the A3 fragment of chromosome 14 fused to the E3 region derived from chromosome 15 as well as a product derived from chromosome 15 that had lost the E3 region in the same metaphase (Figure 6c, d) unequivocally

demonstrated the presence of a reciprocal T(14;15) translocation in CarC-R, as found previously in CarC and CarC-RT-derived cell clones by SKY. The dual color metaphase FISH also revealed that T(14;15) was absent from premalignant MCA3D keratinocytes (data not shown), which are nontumorigenic upon injection in nude mice (Quintanilla *et al*., 1991), and served as a negative control. A summary of the detection of T(14;15) by FISH in CarC-R, CarC-RT and CarC cells is presented in Table 3. Overall, the data of Tables 2 and 3 indicated that only 1.9% of CarC-R cells contained the T(14;15) translocation (5 out of 263 metaphases), while it was widely distributed in CarC-RT and CarC cell populations with more than 90% of metaphases displaying T(14;15). The above results indicate that T(14;15) translocation segregates with tumorigenicity, since it was present in only a minority of CarC-R cells that were selected *in vivo* in the mouse to produce a tumor.

Discussion

In this report, we have characterized a cell subpopulation (CarC-R) contained in a spindle carcinoma cell line (CarC) derived from a chemically-induced mouse skin tumor. CarC-R cells are epithelial *in vitro* and exhibit a drastic reduction in their tumorigenic properties when compared with CarC, yet they are phenotypically plastic *in vivo*, producing sarcomatoid carcinomas with only small (< 5%) epithelial cell components. Similarly, cell lines with an unstable phenotype, capable of eliciting a reversible EMT *in vitro* and *in vivo*, have been previously obtained by others, generally derived from primary tumors containing mixed spindle and epithelial cell components (Buchmann *et al*., 1991; Portella *et al*., 1998).

Both CarC-R and CarC cell lines contain the same DMBA-specific A-T mutation at codon 61 of the *H-Ras* gene, which is associated with initiation of

carcinogenesis (Quintanilla et al., 1986). However, while CarC-R cells retain the normal *H-Ras* allele, it is lost in CarC spindle cells. Increased mutant to normal H-Ras ratios (or loss of the normal H-Ras allele) is a frequent characteristic associated with the SCC-SpCC transition *in vivo* (Buchmann *et al*., 1991). Thus, fibroblastic cell clones derived from an explanted CarC-R tumor (CarC-RT) tended to express increased mutant to normal *H-Ras* transcript levels in comparison with epithelial cell clones derived from the same tumor. In particular, reduced expression of normal *H-Ras* was more evident in F2 cells. *H-Ras* is considered a major driving force for tumor progression in mouse skin carcinogenesis. The mutant *H-Ras* allele is frequently duplicated in papillomas and amplified to multiple copies or overexpressed in SCCs (Bremner and Balmain, 1990; Bianchi *et al*., 1990; Rodriguez-Puebla *et al*., 1999). Thus, successive increases in Ras activity appear to correlate with malignant potential, but this model requires down-regulation or loss of downstream signals that would lead to growth arrest or cell death by enhanced Ras oncogenic activity, such as p16INK4a and p19INK4a/ARF (Frame and Balmain, 2000). In fact, deletions in the INK4 locus are frequent events associated with the late spindle stage of tumor progression, and CarC cells were found to have deleted the *p15INK4b* and *p16INK4a* genes (Linardopoulos *et al*., 1995). The *INK4a* locus encodes two transcripts, *p16* and *p19*, originating from an alternate first exon and common second and third exons (Duro *et al*., 1995; Mao *et al*., 1995; Stone *et al*., 1995). The finding that CarC spindle cells do not express *p16* and *p19* genes indicates that they have deleted the entire *INK4a* locus. In contrast, CarC-R cells express *p19* mRNA and protein, but they have silenced *p16* transcriptional activity, likely by promoter methylation. These results suggest that sequential inactivation of *p16* and *p19* occurs at later stages of tumor progression, the latter associated with the acquisition of a full malignant phenotype. This important role of *p19* in malignancy is confirmed by

genetically engineered mouse models, where the inactivation of p19, but not p16, predispose to the development of spontaneous tumors (reviewed in Serrano, 2000; Sherr, 2001). In particular, regarding the susceptibility of these mice to DMBA-induced carcinogenesis, *p16*-deficient mice showed a similar frequency of skin tumors than wild-type mice (Sharpless *et al*., 2001), while in *p19*-deficient mice the number and growth rate of papillomas was increased, and progression to highly aggressive spindle cell carcinomas was accelerated (Kelly-Spratt *et al*., 2004).

In addition to the above genetic alterations, we have identified in this work a reciprocal T(14;15) translocation, which is widely distributed in the CarC cell population, but present in only a minority (1.9 %) of CarC-R cells. T(14;15) is selected *in vivo* in tumors induced by CarC-R in nude mice, indicating that it is associated with malignancy. The fact that T(14;15) segregates with both epithelial and fibroblast clonal derivatives of CarC-RT indicates that it is not related to a particular phenotype. Although a T(14;15) was observed in a spontaneous thymic lymphoma developed in a mouse deficient for both histone H2AX and p53 (Celeste *et al*., 2003), to our knowledge T(14;15) translocations have not been found before in mouse epithelial tumors. The chromosome 15 breakpoint was mapped between clones RP23-236P20 (region D1) and RP23-6B22 (region D3), still separated by a long distance of approximately 17 Mb. Further studies are in progress to delineate the precise location of breakpoints in chromosomes 15 and 14, and to determine whether rearrangements of specific genes are involved in the translocation. In this respect, we have not observed significant changes in the expression of *c-myc* in the cell lines that could be related to this translocation (data not shown). *c-myc* is located in band D2 of chromosome 15, the region where T(14;15) appears to occur, and is involved in recurrent T(15;12) translocations

associated with pro-B cell lymphomas (Celeste *et al*., 2003; Difilippantonio *et al*., 2002).

The finding that CarC and CarC-R cell lines carry the same mutation at the *H-Ras* gene, together with the presence of the same T(14;15) translocation and absence of mutations in the central core of the *p53* gene argues in favour of a common origin, likely clonal for both cell lines. Furthermore, CarC-R appears to represent a stage previous to CarC in malignant progression, as suggested by their respective tumorigenic and phenotypic characteristics and the presence in CarC of additional genetic alterations; i.e., loss of the normal *H-Ras* allele, deletion of the INK4a/ARF locus and spread of T(14;15). Nevertheless, the relationship between these two cell lines is not clear at present. CarC-R cells with a near-triploid (61-70) number of chromosomes are aneuploid and exhibit a wide variety of chromosomal aberrations. In contrast, most of CarC cells are near-diploid or near-tetraploid and are characterized by a single specific T(14;15) chromosomal translocation (and by a secondary T(11;19) translocation which is present in only about 25% of the cells). These results support previous reports showing an intimate relationship between chromosomal instability and the degree of aneuploidy (Lengauer *et al*., 1997; Lengauer *et al*., 1998; Miyoshi *et al*., 2000; Beheshti *et al*., 2001; Takahashi *et al*., 1999). Both events appear to occur early in tumorigenesis and precede malignant transformation (Duesberg *et al*., 1998; Duesberg *et al*., 1999; Shih *et al*., 2001). CarC cells could derive from the small CarC-R cell subpopulation that contains the T(14;15) translocation. Since no cell with T(14;15) could be found in CarC-R by SKY, it was not possible to determine whether these minority CarC-R cell subpopulation was aneuploid, like the vast majority of CarC-R cells, or near-diploid/tetraploid as CarC. However, *in vivo* selection of CarC-R cells containing T(14;15) appears to indicate that these cells are in fact aneuploid, as seen by the

karyotypes displayed by CarC-RT-derived cell clones. Therefore, the prospect that CarC cells have evolved from a highly aneuploid, genetically unstable CarC-R cell subpopulation would imply that, at least in some cases, the degree of aneuploidy declines during the latest stages of tumor progression. It is thought that karyotypic instability would accelerate the rate of mutation in dividing cancer cells, generating in a stochastic manner new abnormal and heterogeneous karyotypes, most of which would be lethal. Cells containing a more balanced number of chromosomes and fixed genetic alterations conferring a growth advantage; i.e., increased mutant to normal *H-Ras* gene dosage, *p16INK4a* and *p19ARF* gene inactivation, and T(14;15), might have been selected for tumor progression with each wave of clonal expansion. Further studies within this cell model will test the feasibility of this hypothesis.

Materials and Methods

Cell lines, culture conditions and drug treatment

To obtain the CarC-R cell line, CarC cells (p. > 50) were seeded at low density in 100 mm plastic dishes, and a colony of cells displaying an epithelial morphology (CarC-R) was isolated by a cloning ring. CarC-R cells were grown, expanded to several flasks, and frozen. The CarC-RT cell line was isolated from an explanted tumor induced by s.c. injection of CarC-R cells into the back of a nude mouse. Clones F2, F3, F4, F5, E1, E2, E4 were isolated from an early passage (p. 2) CarC-RT cell culture by cloning rings. Other cell lines used in this work were premalignant MCA3D and transformed PDV mouse keratinocytes (Kulesz-Martin *et al*., 1983, Fusenig *et al*., 1978).

Cells were grown in Ham's F-12 medium supplemented with amino acids and vitamins (MCA3D, PDV) or Dulbecco's modified Eagle's medium (CarC, CarC-R,

CarC-RT cells and CarC-RT-derived clones), in the presence of 10% fetal calf serum (Gibco Invitrogen Corp., Barcelona, Spain) and antibiotics (100 μg/ml ampicillin, 32 μg/ml gentamicin; 25 μg/ml amphotericin B; Sigma-Aldrich, Madrid, Spain). Cultures were maintained at 37 °C in a 5% CO_2 humidified atmosphere.

The methyltransferase inhibitor 5-aza-dC (Sigma-Aldrich) was used to test the effect of demethylation on *p16* gene expression. Cells were treated with either 10 μM 5-aza-dC or the same volume of ethanol (used as a solvent for the drug) for 48 h. After treatment, cells were washed in PBS and harvested for Western blot analysis.

RT-PCR analysis

RNA samples (2 μg) isolated from the cell lines by the guanidinium thiocyanate procedure were incubated with the Moloney murine leukemia virus reverse transcriptase (Promega Corp., Madison, WI, USA), and the generated cDNAs were used for PCR amplification. For specific detection of mouse *p16* and *p19* mRNAs, we used oligonucleotides to amplify fragments corresponding to exon 1α (133-bp) and exon 1β (205-bp) of the *INK4a* locus, as well as primers to amplify the entire coding region of *p16* (516-bp) and *p19* (586-bp). For mouse *H-Ras*, oligonucleotides to amplify a cDNA fragment containing the codon 61 were used. The 400-bp product was isolated using a gel extraction kit (QIAquick; QuiagenGmbH, Hilden, Germany). The presence of a DMBA-specific A-T mutation at codon 61 was verified by digestion of the DNA with *XbaI* (Gibco Invitrogen Corp.), as previously reported (Quintanilla et al., 1986). For *p53*, oligonucleotides to amplify a cDNA fragment containing exons 3-9 were used. The 928-bp product was isolated and directly sequenced in an ABI PRISM 377 machine (PE Applied Biosystems, Foster city, CA, USA). See *Supplementary Information* for specific primers and PCR conditions.

Western blot analysis

Specific proteins were detected by using enhanced chemiluminiscence (Amersham Corporation, Arlington Heights, FL) and the following primary antibodies: rabbit polyclonal anti-p16 (1:250) (Santa Cruz Biotechnology Inc., Santa Cruz, CA, USA), rabbit polyclonal anti-p19 (1:500) (raised against amino acids 54-75; kindly provided by Dr. I. Palmero, Instituto de Investigaciones Biomédicas, CSIC-UAM, Madrid, Spain) and mouse monoclonal anti-α-tubulin DM1A (1:10000) (Sigma Aldrich). As secondary antibodies, anti-mouse or anti-rabbit IgGs coupled to horseradish peroxidase (Nordic Immunological laboratories, Tilburg, The Netherlands) were used.

Cytogenetic studies, spectral karyotyping and fluorescence *in situ* hybridization analysis

For conventional cytogenetic analysis, cells were exposed to colchicine (0.5 μg/ml) for 6 h at 37ºC, and harvested routinely. Metaphases were analyzed after standard Giemsa staining, C-banded and DAPI staining, as described (Bella *et al*., 1995).

For SKY analysis, slide preparation and hybridization, using commercial probes, were carried out according to the manufacturer's instructions (Applied Spectral Imaging [ASI], Migdal Ha'Emek, Israel). Images were acquired using an ASI SD300 Spectracube mounted on a Zeiss Axioplan 2 microscope.

For FISH studies, Ensembl Cytoview was used to select BAC clones covering regions C, D1, D3 and E3 from chromosome 15, and region A3 from chromosome 14. Clones were purchased from the Children Hospital Oakland Research Institute (CHORI; www.chori.org/bacpac/) and used for FISH analysis. All BACs were labelled directly

by nick translation with SpectrumGreen- or SpectrumOrange-dUTPs, according to the manufacturer's specifications (Vysis, Dowers Grove, IL, USA). The probes were blocked with mouse Cot-1 DNA (Gibco Invitrogen Corp.) to suppress repetitive sequences. Metaphase spreads from the cell lines were hybridized overnight at 37ºC with labelled probes. After post-hybridization washes, the chromosomes were counterstained with DAPI in antifade solution. Cell images were captured using a CCD camera (Photometrics SenSys camera) connected to a computer running the Chromofluor image analysis system (Cytovision, Applied Imaging Ltd, Newcastle, UK).

Tumorigenicity assay

For tumorigenicity assays, $3x10^6$ viable cells were i.d. injected into the two flanks of 8-week-old female athymic BALB/c nude mice (Harlan S. L., Barcelona, Spain). The latency period was estimated as the time needed for tumors to reach a size of 1-cm^2. Histological typing of developed tumors was performed in formalin-fixed and paraffin-embedded sections by staining with hematoxylin and eosin.

Acknowledgements

We thank Dr. Ignacio Palmero for his generous gift of anti-p19 antibody and helpful suggestions during the course of this work, and Maria M. Yurrita for critical reading of the manuscript. This study was supported by grants from the "Ministerio de Educación y Ciencia" of Spain (SAF2004-04902) and "Fondo de Investigación Sanitaria" (Red de Centros de Cáncer, RTICCC, CO3/10) to MQ, and by the European Union (Cost Action B19, "Molecular Cytogenetics of Solid Tumours") to JCC. MP and

SR-P were the recipients of fellowships from the “Ministerio de Educación y Ciencia” and “Fundación Inocente Inocente” of Spain, respectively.

References

Akhurst RJ and Balmain A. (1999). *J. Pathol.*, **187**, 82-90.

Aldaz CM, Conti CJ, Klein-Szanto AJ and Slaga TJ. (1987). *Proc. Natl. Acad. Sci. U S A*, **84**, 2029-2032.

Aldaz CM, Trono D, Larcher F, Slaga TJ and Conti CJ. (1989). *Mol. Carcinog.*, **2**, 22-26.

Beheshti B, Park PC, Sweet JM, Trachtenberg J, Jewett MA and Squire JA. (2001). *Neoplasia*, **3**, 62-69.

Bella JL, Fernandez JL and Gosalvez J. (1995). *Genome*, **38**, 864-868.

Bianchi AB, Aldaz CM and Conti CJ. (1990). *Proc. Natl. Acad. Sci. U S A*, **87**, 6902-6.

Bremner R and Balmain A. (1990). *Cell*, **61**, 407-417.

Buchmann A, Ruggeri B, Klein-Szanto AJ and Balmain A. (1991). *Cancer Res.*, **51**, 4097-4101.

Burns PA, Kemp CJ, Gannon JV, Lane DP, Bremner R and Balmain A. (1991). *Oncogene*, **6**, 2363-2369.

Celeste A, Difilippantonio S, Difilippantonio MJ, Fernandez-Capetillo O, Pilch DR, Sedelnikova OA, Eckhaus M, Ried T, Bonner WM and Nussenzweig A. (2003). *Cell*, **114**, 371-383.

Conti CJ, Aldaz CM, O'Connell J, Klein-Szanto AJ and Slaga TJ. (1986). *Carcinogenesis*, **7**, 1845-1848.

Diaz-Guerra M, Haddow S, Bauluz C, Jorcano JL, Cano A, Balmain A and Quintanilla M. (1992). *Cancer Res.*, **52**, 680-687.

Difilippantonio MJ, Petersen S, Chen HT, Johnson R, Jasin M, Kanaar R, Ried T and Nussenzweig A. (2002). *J. Exp. Med.*, **196**, 469-480.

Duesberg P, Rasnick D, Li R, Winters L, Rausch C and Hehlmann R. (1999). *Anticancer Res.*, **19**, 4887-4906.

Duesberg P, Rausch C, Rasnick D and Hehlmann R. (1998). *Proc. Natl. Acad. Sci. U S A*, **95**, 13692-13697.

Duro D, Bernard O, Della Valle V, Berger R and Larsen CJ. (1995). *Oncogene*, **11**, 21-29.

Frame S and Balmain A. (2000). *Curr. Opin. Genet. Dev.*, **10**, 106-113.

Frame S, Crombie R, Liddell J, Stuart D, Linardopoulos S, Nagase H, Portella G, Brown K, Street A, Akhurst R and Balmain A. (1998). *Philos. Trans. R. Soc. Lond. B. Biol. Sci.*, **353**, 839-845.

Fusenig NE, Amer SM, Boukamp P and Worst PK. (1978). *Bull. Cancer*, **65**, 271-279.

Gotzmann J, Mikula M, Eger A, Schulte-Hermann R, Foisner R, Beug H and Mikulits W. (2004). *Mutat. Res.*, **566**, 9-20.

Grady WM. (2004). *Cancer Metastasis Rev.*, **23**, 11-27.

Kelly-Spratt KS, Gurley KE, Yasui Y and Kemp CJ. (2004). *PLoS. Biol.*, **2**, E242.

Klein-Szanto AJ, Larcher F, Bonfil RD and Conti CJ. (1989). *Carcinogenesis*, **10**, 2169-2172.

Kulesz-Martin M, Kilkenny AE, Holbrook KA, Digernes V and Yuspa SH. (1983). *Carcinogenesis*, **4**, 1367-1377.

Lengauer C, Kinzler KW and Vogelstein B. (1997). *Nature*, **386**, 623-627.

Lengauer C, Kinzler KW and Vogelstein B. (1998). *Nature*, **396**, 643-649.

Linardopoulos S, Street AJ, Quelle DE, Parry D, Peters G, Sherr CJ and Balmain A. (1995). *Cancer Res.*, **55**, 5168-5172.

Mao L, Merlo A, Bedi G, Shapiro GI, Edwards CD, Rollins BJ and Sidransky D. (1995). *Cancer Res.*, **55**, 2995-2997.

Miyoshi Y, Iwao K, Takahashi Y, Egawa C and Noguchi S. (2000). *Cancer Lett.*, **159**, 211-216.

Navarro P, Gomez M, Pizarro A, Gamallo C, Quintanilla M and Cano A. (1991). *J. Cell. Biol.*, **115**, 517-533.

Pihan GA and Doxsey SJ. (1999). *Semin. Cancer Biol.*, **9**, 289-302.

Portella G, Cumming SA, Liddell J, Cui W, Ireland H, Akhurst RJ and Balmain A. (1998). *Cell Growth Differ.*, **9**, 393-404.

Quelle DE, Zindy F, Ashmun RA and Sherr CJ. (1995). *Cell*, **83,** 993-1000.

Quintanilla M, Brown K, Ramsden M and Balmain A. (1986). *Nature*, **322**, 78-80.

Quintanilla M, Haddow S, Jonas D, Jaffe D, Bowden GT and Balmain A. (1991). *Carcinogenesis*, **12**, 1875-1881.

Rajagopalan H, Nowak MA, Vogelstein B and Lengauer C. (2003). *Nat. Rev. Cancer*, **3**, 695-701.

Rodriguez-Puebla ML, LaCava M, Bolontrade MF, Russell J and Conti CJ. (1999). *Mol. Carcinog.*, **26**, 150-156.

Ruas M and Peters G. (1998). *Biochim. Biophys. Acta.*, **1378**, F115-F177.

Ruggeri B, Caamano J, Slaga TJ, Conti CJ, Nelson WJ and Klein-Szanto AJ. (1992). *Am. J. Pathol.*, **140**, 1179-1185.

Serrano M. (2000). *Carcinogenesis*, **21**, 865-869.

Sharpless NE, Bardeesy N, Lee KH, Carrasco D, Castrillon DH, Aguirre AJ, Wu EA, Horner JW and DePinho RA. (2001). *Nature*, **413**, 86-91.

Sherr CJ. (2001). *Nat. Rev. Mol. Cell Biol.*, **2**, 731-737.

Shih IM, Zhou W, Goodman SN, Lengauer C, Kinzler KW and Vogelstein B. (2001). *Cancer Res.*, **61**, 818-822.

Stoler AB, Stenback F and Balmain A. (1993). *J. Cell. Biol.*, **122**, 1103-1117.

Stone S, Jiang P, Dayananth P, Tavtigian SV, Katcher H, Parry D, Peters G and Kamb A. (1995). *Cancer Res.*, **55**, 2988-2994.

Takahashi T, Haruki N, Nomoto S, Masuda A, Saji S and Osada H. (1999). *Oncogene*, **18**, 4295-4300.

Thiery JP. (2002). *Nat. Rev. Cancer*, **2**, 442-454.

Vousden KH and Lu X. (2002). *Nat. Rev. Cancer*, **2,** 594-604.

Yuspa SH, Dlugosz AA, Cheng CK, Denning MF, Tennenbaum T, Glick AB and Weinberg WC. (1994). *J. Invest. Dermatol.*, **103**, 90S-95S.

Legends to figures

Figure 1. Phase-contrast micrographs of the different cell lines. Bars, 100 μm.

Figure 2. Histological appearance of tumors induced by CarC (**a** and **c**) and CarC-R (**b** and **d**) in nude mice. Panels **c** and **d** show higher magnifications of sarcomatoid and epithelial differentiation areas, respectively. Note that tumors induced by both cell lines are highly undifferentiated, but the CarC-R tumor of panel **b** contains a small region of epithelial cell differentiation (marked with a dotted line) showed in panel **d** at a higher magnification.

Figure 3. Characterization of *H-Ras* and *INK4a* gene expression. (**a**) Expression of normal and mutated *H-Ras* genes. A 400-bp mRNA product containing the codon 61 of murine *H-Ras* was amplified by RT-PCR using specific primers. The products were run on agarose-ethidium bromide gels before (*upper* panel) and after (*middle* panel) digestion with *XbaI*. Mutation of the middle base of codon 61 from A to T gives rise to a *XbaI* restriction site, generating fragments of 262-bp and 138-bp; n, normal *H-Ras* undigested with the enzyme; m, mutated *H-Ras*. Amplification of *GAPDH* mRNA was used as a control (*bottom* panel). Note in the *middle* panel that the relative band intensities of mutated *versus* normal fragments are increased in the fibroblastic (F3, F4, F5, F2) with respect to the epithelial (E2, E1, E4) cell clones. (**b**, **c**) Expression of *p16INK4a* and *p19ARF* genes by RT-PCR (**b**) and Western blotting (**c**). Immunodetection of α-tubulin was used as a control for protein loading. (**d**) Induction of p16 expression by the demethylating agent 5-aza-dC. Representative Western blot of p16 protein expression after a 48 h treatment of CarC and CarC-R cells with 10 μM 5-

aza-dC or solvent (- 5-aza-dC). The PDV carcinoma cell line which contains a 2:1 ratio of normal to mutated *H-Ras* alleles (Quintanilla *et al*., 1991) and expresses *p16* and *p19* genes was used as a positive control for all these experiments.

Figure 4. Distribution of chromosome numbers of CarC and CarC-R cell lines. A total of 52 and 51 metaphases were analyzed in CarC and CarC-R, respectively.

Figure 5. Spectral karyotypes from CarC and CarC-R cell lines. (**a**) SKY karyotype from a representative diploid CarC cell. Each chromosome pair is represented by a DAPI banded image (white box on the *left*) and the classified spectrum image (to the *right* of the banded image). (**b**) Detail of the reciprocal translocation between chromosome 14 and 15, which appears as two-coloured chromosomes. (**c**) SKY karyotype from a representative near-triploid CarC-R cell. Each chromosome is also represented by two images as in panel **a**. Several chromosome aberrations, such as dicentric chromosome 3;18, translocations involving chromosomes 4, 10, and 13, and amplifications involving chromosomes 11 and 12, are indicated.

Figure 6. FISH analysis of the t(14;15) translocation. (**a**) Labelling scheme for detecting translocated chromosomes: a normal chromosme 15 appears with four hybridisation signals with the sequence green-red-green-red from centromere to telomere. The appearance of only two green-red signals indicates the presence of a translocated chromosome 14 or 15. (**b**) Metaphase spread from a CarC-R cell showing five normal chromosomes 15 and two translocated chromosomes (encircled in white). (**c**) Labelling scheme for detecting translocated chromosomes: a normal chromosome 15 appears with two hybridisation signals with the sequence green-red from centromere to

telomere, while a normal chromosome 14 appears with a diffuse large green signal close to the centromere. Translocated chromosome 15 appears with a single green signal and translocated chromosome 14 appears with the diffuse large green signal and the additional more telomeric red signal from chromosome 15. (**d**) Metaphase spread from a CarC-R cell showing normal chromosomes 14 and 15 and translocated products (encircled in white). The finding of a der(15)T(14;15) and a der(14)T(14;15) within the same cell strongly suggests the presence of a reciprocal translocation involving chromosomes 14 and 15.

Table 1 p53 mutations found in the cell lines[a]

Cell line	*Mutation*
PDV	Codon 234 ATG→GTG
CarC	None
CarC-R	None
F4	None
F2	None
E2	None
E4	None

[a]Exons 3–9 of the *p53* gene were amplified by RT–PCR and directly sequenced

Table 2 Summary of the spectral karyotype of the cell lines

Cell line	*No. of analysed metaphases*	*SKY karyotype (only structural aberrations)*
CarC	17	38–42, X, T(14;15) 38–42, X, T(14,15), T(11;19) (25%) 63–65, XXX, T(14;15) 80–84, XXXX, T(14;15)
CarC-R	63	60–68, Del(X), T(2,3), Rb(3.18), T(4;10), Is(10;13;4), Hsr(11)
F2	18	75–98, Del(X), Del(2), T(2;3), Rb(3.18), T(9;19), Hsr(11), T(14;15), Rb(7.17)
F4	10	68–102, Del(X), Rb(3.18), T(4;10), Is(10;13;4), Rb(6.10), T(5;18), T(X;8;11), Hsr(11), T(1;9), T(14;15), Rb(17.17)
E2	8	74–91, T(2;3), Rb(3.18), T(4;10), Is(10;13;4), Hsr(11), T(14;15)
E4	10	65–108, Del(X), T(X;X), T(2;3), T(4;10), Hsr(11), T(14;15)

Table 3 Summary of the presence of T(14;15) in the cell lines, as determined by FISH analysis

Cell line	*No. of analysed metaphases*	*No. of metaphases containing T(14;15)*
CarC-R	200	5
CarC-RT	10	9
CarC	5	5

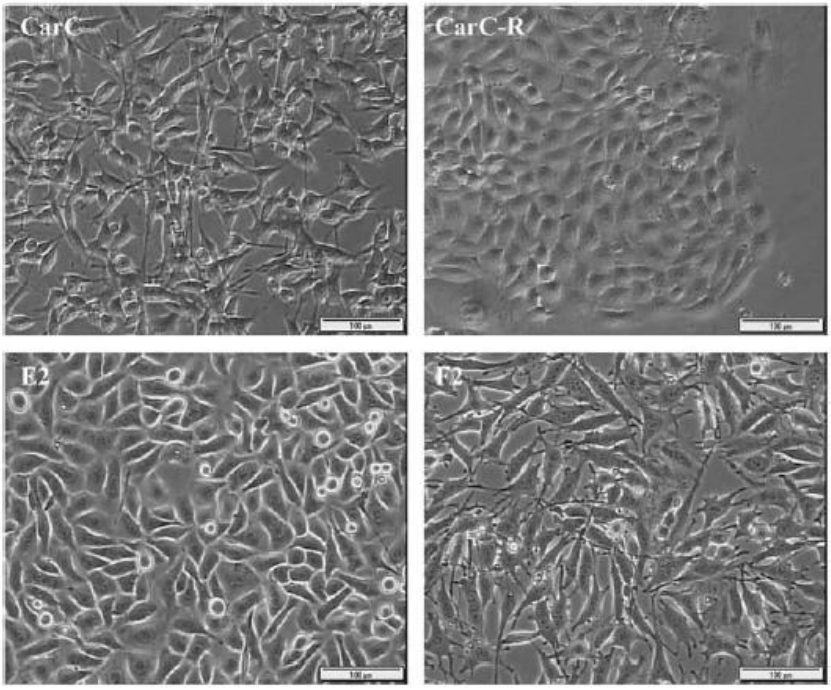

Figure 1 Phase-contrast micrographs of the different cell lines. Bars, 100 μm

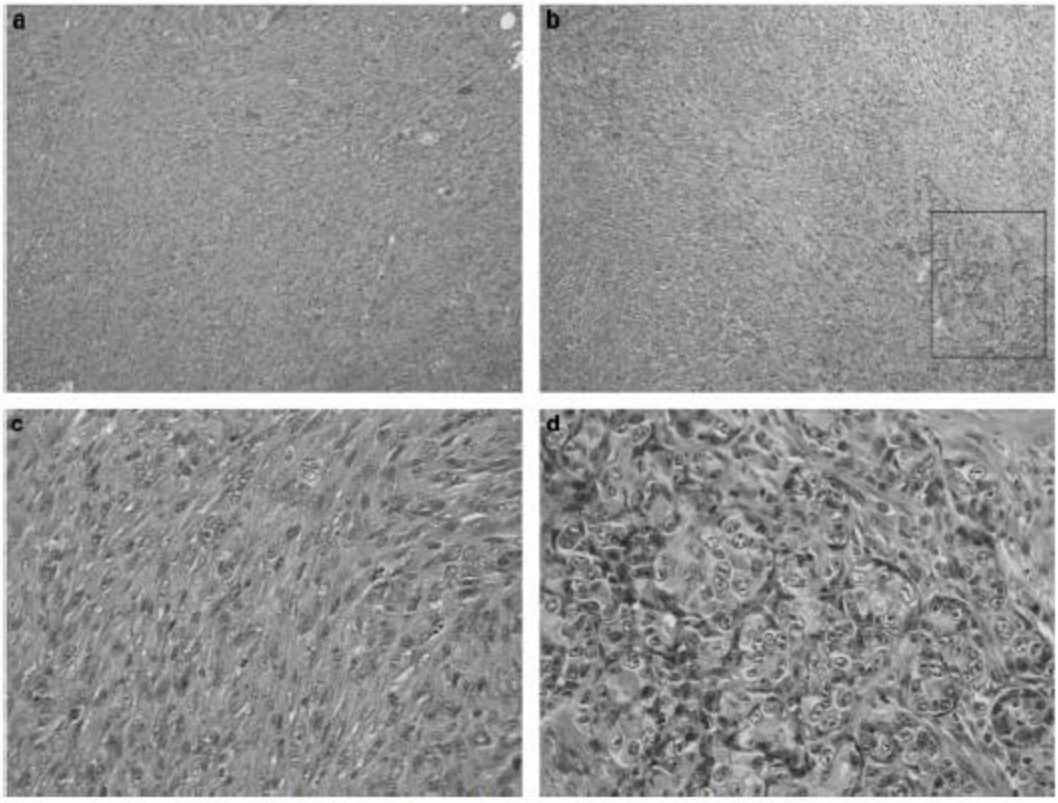

Figure 2 Histological appearance of tumors induced by CarC (**a** and **c**) and CarC-R (**b** and **d**) in nude mice. Panels c and d show higher magnifications of sarcomatoid and epithelial differentiation areas, respectively. Note that tumors induced by both cell lines are highly undifferentiated, but the CarC-R tumor of panel b contains a small region of epithelial cell differentiation (marked with a dotted line) showed in panel d at a higher magnification

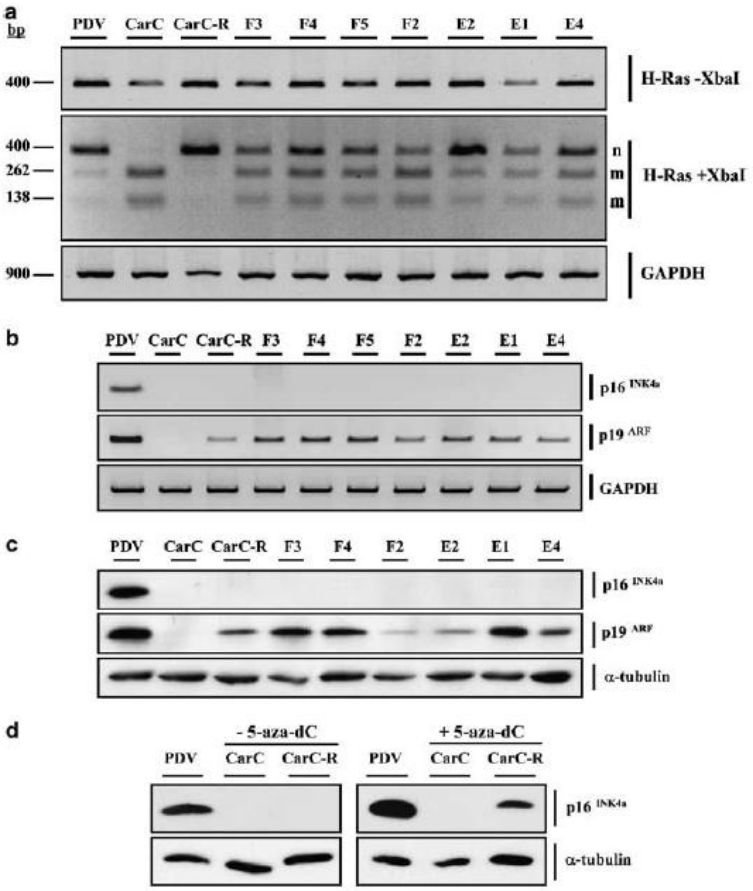

Figure 3 Characterization of *H-Ras* and *INK4a* gene expression. (**a**) Expression of normal and mutated *H-Ras* genes. A 400-bp mRNA product containing the codon 61 of murine *H-Ras* was amplified by RT–PCR using specific primers. The products were run on agarose–ethidium bromide gels before (upper panel) and after (middle panel) digestion with *Xba*I. Mutation of the middle base of codon 61 from A to T gives rise to a *Xba*I restriction site, generating fragments of 262 and 138 bp; n, normal *H-Ras* undigested with the enzyme; m, mutated *H-Ras*. Amplification of *GAPDH* mRNA was used as a control (bottom panel). Note in the middle panel that the relative band intensities of mutated *versus* normal fragments are increased in the fibroblastic (F3, F4, F5, F2) with respect to the epithelial (E2, E1, E4) cell clones. (**b** and **c**) Expression of *p16INK4a* and *p19ARF* genes by RT–PCR (**b**) and Western blotting (**c**). Immunodetection of α-tubulin was used as a control for protein loading. (**d**) Induction of *p16* expression by the demethylating agent 5-aza-dC. Representative Western blot of p16 protein expression after a 48 h treatment of CarC and CarC-R cells with 10 μM 5-aza-dC or solvent (−5-aza-dC). The PDV carcinoma cell line that contains a 2 : 1 ratio of normal to mutated *H-Ras* alleles (Quintanilla *et al.*, 1991) and expresses *p16* and *p19* genes was used as a positive control for all these experiments

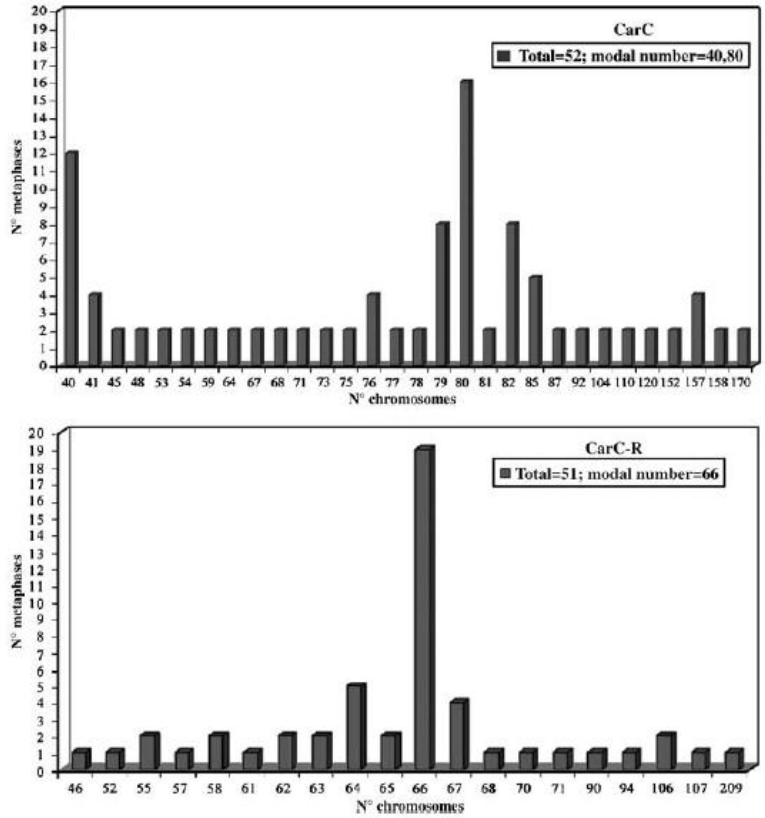

Figure 4 Distribution of chromosome numbers of CarC and CarC-R cell lines. A total of 52 and 51 metaphases were analysed in CarC and CarC-R, respectively

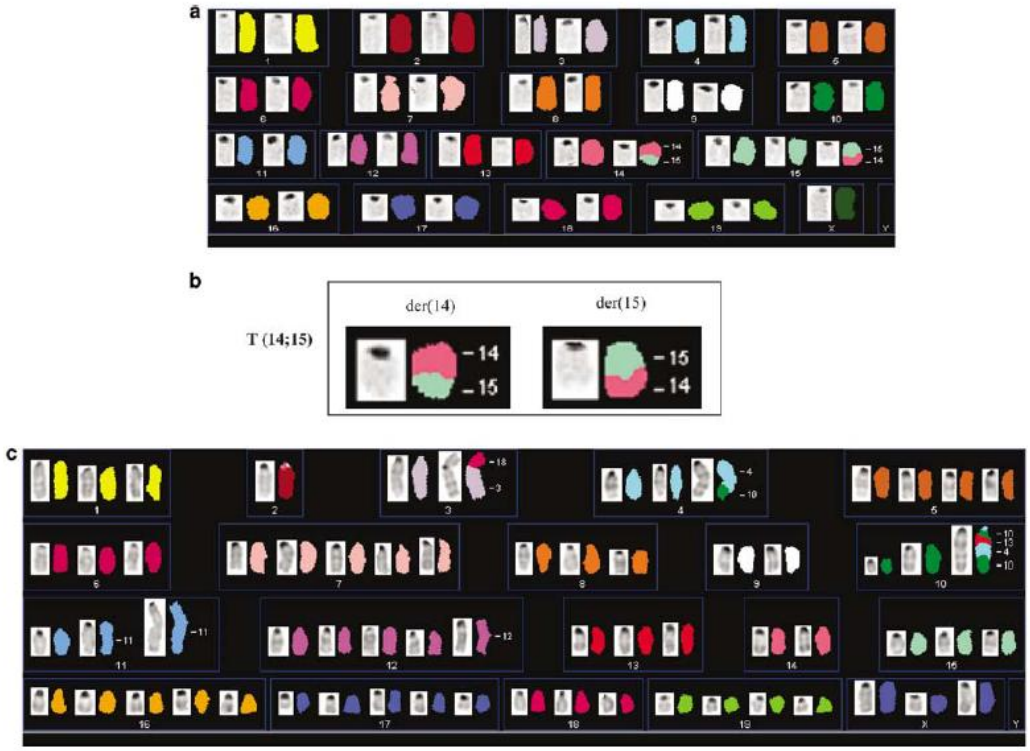

Figure 5 Spectral karyotypes from CarC and CarC-R cell lines. (**a**) SKY karyotype from a representative diploid CarC cell. Each chromosome pair is represented by a DAPI-banded image (white box on the *left*) and the classified spectrum image (to the *right* of the banded image). (**b**) Details of the reciprocal translocation between chromosomes 14 and 15, which appears as two-colored chromosomes. (**c**) SKY karyotype from a representative near-triploid CarC-R cell. Each chromosome is also represented by two images as in panel a. Several chromosome aberrations, such as dicentric chromosome 3;18, translocations involving chromosomes 4, 10 and 13, and amplifications involving chromosomes 11 and 12, are indicated

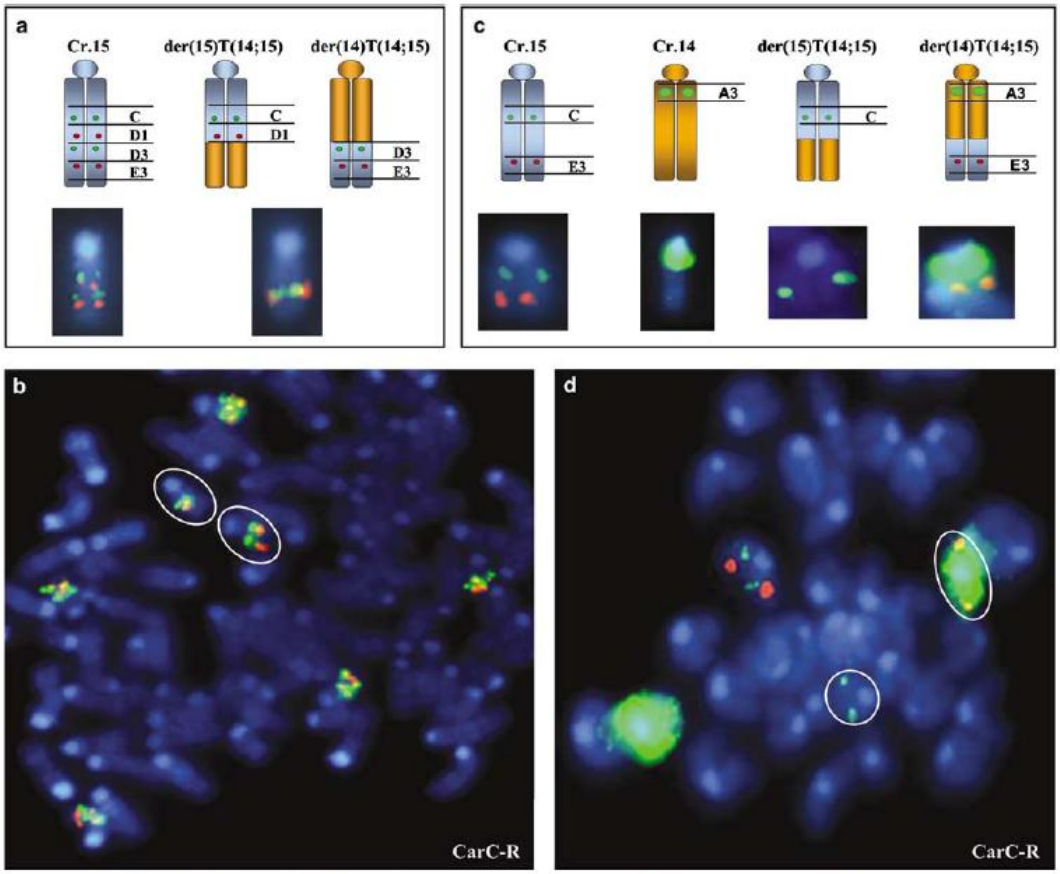

Figure 6 FISH analysis of the T(14;15) translocation. (**a**) Labeling scheme for detecting translocated chromosomes: a normal chromosme 15 appears with four hybridization signals with the sequence green-red-green-red from centromere to telomere. The appearance of only two green-red signals indicates the presence of a translocated chromosome 14 or 15. (**b**) Metaphase spread from a CarC-R cell showing five normal chromosome 15 and two translocated chromosomes (encircled in white). (**c**) Labeling scheme for detecting translocated chromosomes: a normal chromosome 15 appears with two hybridization signals with the sequence green-red from centromere to telomere, while a normal chromosome 14 appears with a diffuse large green signal close to the centromere. Translocated chromosome 15 appears with a single green signal and translocated chromosome 14 appears with the diffuse large green signal and the additional more telomeric red signal from chromosome 15. (**d**) Metaphase spread from a CarC-R cell showing normal chromosomes 14 and 15 and translocated products (encircled in white). The finding of a der(15)T(14;15) and a der(14)T(14;15) within the same cell strongly suggests the presence of a reciprocal translocation involving chromosomes 14 and 15